Gold nanoshells aided optical imaging *in vitro, in vivo*, and *ex vivo*

M. Lee[*1], C. Loo[**1], A. M. Gobin[***], J. Park[*], J. West[***], N. Halas[***], and R. Drezek[***]

[*]Korea Electronics Technology Institute
68 Yatapdong, Bundang gu, Gyeong-gi do 463-816, Korea mhlee@keti.re.kr
[**]Baylor College of Medicine, TX, USA
[***]Rice University, Houston, TX, USA
[1]equal contribution

ABSTRACT

Scatter-based optical imaging technologies such as Optical Coherence Tomography (OCT) and Reflectance Confocal Microscopy (RCM) offer a unique non-invasive approach to the detection, diagnosis, and monitoring of cancer. In this article, we describe the use of targeted NIR-tuned gold nanoshell for imaging *in vitro, ex vivo* and *in vivo*. Nanoshells are a new class of optically active nanoparticles with tunable plasmon resonances based on geometric construction. These particles can be easily tuned to absorb or scatter strongly within the wavelengths of 650-1300 nm, known as the near infrared region. This region is of significant biological importance providing a therapeutic window and imaging applications in tissue as the primary components of tissue, blood and water, do not have significant absorption coefficients in this range of wavelengths.

Keywords: nanoshells, optical imaging, plasmon

1 INTRODUCTION

Scatter-based optical imaging offers a novel approach to biomedical imaging. Imaging modalities such as Optical Coherence Tomography (OCT) and Reflectance Confocal Microscopy (RCM) offer the potential for non-invasive high-resolution, real-time imaging at competitive costs. However, these techniques have limited sensitivity since scattering contrast highly relies on inherent changes in refraction [1]. Optical imaging based on the presence of disease specific molecular markers may prove highly beneficial in the area of early cancer detection [2]. Contrast agents possessing inherent optical properties and targeted to these markers would improve the contrast that would otherwise be normally undetectable. Moreover, the near infrared (NIR) region is of particularly interest for biomedical imaging applications because this is the spectral region where tissue is most optically transparent, allowing for deeper structures to be imaged [3]. Tunable NIR contrast agents, targeted to disease-specific molecular markers would be greatly beneficial whenever these optical imaging strategies are employed. In this paper, we describe the use of a novel class of nanoparticles with optical properties tunable into the NIR, targeted to disease-specific molecular markers for OCT and RCM imaging *in vitro* and *ex vivo*. In addition, OCT images of tumor bearing mouse were taken with scattering gold nanoshells *in vivo*. Gold nanoshells, composed of a dielectric core covered by gold, can be devised for diagnostic purposes by appropriately tuning of their optical properties through modification of nanoshell core-to-shell thickness ratio as well as overall particle size.

2 MATERIALS AND METHODS

2.1 Gold Nanoshells Synthesis

The fabrication protocol developed for nanoshells includes molecular self-assembly and colloid chemistry in aqueous solution [4]. Silica cores were made by the Stöber method which involves the reduction of tetraethylorthosilicate (TEOS, Aldrich) in ethanol. Next, the Stöber nanoparticle was functionalized with aminopropyltriethoxysilane (APTES, Aldrich) resulting in silica cores with attached amine groups. When these functionalized groups were placed in a gold colloid solution, small gold colloids adsorb to the amine group. Small gold colloids (1-3 nm) were fabricated according to the method of Duff and Baiker[5]. Gold colloids were aged for 2 weeks at 4° C and concentrated using a rotary evaporator. Gold colloid provides the nucleation sites for further reduction of gold. As gold reduces onto the colloid, the colloid grows until it coalesces into a complete shell. The amount of gold added during this final reduction stage determines the shell thickness. Gold nanoshell sizes were determined by scanning electron microscopy (SEM) and the absorbance was measured with a spectrophotometer (Cary 5000, Varian).

Antibodies were attached on gold surface using the Orthopyridyl disulfide-PEG-n-hydroxysuccinimide (OPSS-PEG-NHS, MW 2000, Nektar) linker to provide strong stability between antibody and gold surface. Antibodies specific to Her2 were prepared and tethered onto gold nanoshells. As a negative control, non specific antibodies to IgG were prepared. Following antibody conjugation, gold surfaces were modified with PEG-SH to eliminate non-specific protein adsorption and to provide stabilization of gold nanoshells.

2.2 Optical Coherence Tomography (OCT) and Reflectance Confocal Microscopy (RCM)

The OCT system for this study is a fiber-based interferometer with electro-optical piezofiber-based in depth scanning for image acquisition. This type of OCT system is described in detail (16). The light source of this system has a center wavelength of 1310 nm, full width half maximum spectral bandwidth of 50 nm, and output power of 13 mW. The axial and transverse resolutions were measured to be approximately 10 μm and 15 μm, respectively..

Confocal images were acquired with a Lucid inverted reflectance laser scanning confocal microscope equipped with a diode laser and detector with an emission wavelength at 830 nm. All images were taken at the same magnification and power.

2.3 Human Breast Cancer Tissue

Histologically normal and abnormal (invasive carcinoma) fresh frozen tissue samples were obtained from the Cooperative Human Tissue Network and were stored at -80^{o}C. Protocol approval was obtained by the Rice University Institutional Review Board. Her2-status was obtained from accompanying pathology reports. Samples were brought to room temperature, thin tissue sections were made, and OCT and RCM images were taken. Following imaging, sections were injected with labeled nanoshells using a 3 ml, 25 gauge syringe with a 1.5 inch needle in order to ensure equal nanoshell distribution (1mL, 5 × 10^{9}/mL) and incubated with nanoshells for 15 minutes. Sections were then washed with PBS and imaged with OCT and RCM. Remaining samples were immediately frozen in liquid N_2.

2.4 BALBc Mice

BALBc mice were used under an approved protocol of the Institutional Animal Care and Use Committee at Rice University. 150,000 cells of the murine colon carcinoma cell line, CT-26; (ATCC) were inoculated in the right flank of mice in 25 $\mu\ell$ of PBS. Tumors were allowed to grow to ~20 – 30 mm^2. PEGylated nanoshells were injected into the tail vein of the animals 20 hours prior to imaging. A total of 36 animals were inoculated with the cancer cells.

3 RESULTS AND DISCUSSION

OCT images were performed on normal and cancerous breast tissue. Figure 1 shows the results of OCT imaging of normal breast tissue. There is no contrast difference found within three type of control normal tissue (top row, normal control) and also no image contrast was observed between with antibody labeled (Her2 and IgG) nanoshells addition and normal controls (top and middle row of Figure 1). Same sets of experiments were performed in malignant tissue with nanoshells.

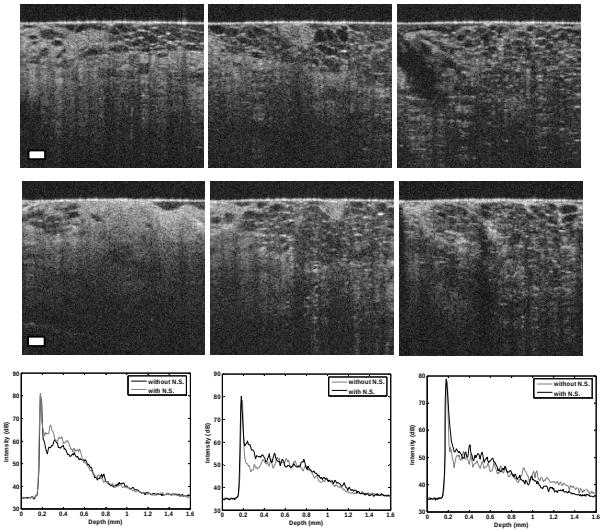

Figure 1: OCT imaging of normal breast tissue *ex vivo*. Histologically normal breast tissue before and after nanoshell addition (top & middle row, respectively). Averaged A-scan images of each column (bottom row). Scale bar is ~200 μm.

Figure 2 shows OCT images of HER2- positive malignant breast tissues without nanoshells (malignant controls) and following with antibody conjugated (HER2 and IgG) nanoshells and with bare nanoshells. There are considerable structural differences observable in structure between normal (Figure 1) and malignant tissues (Figure 2) due to neoplastic changes associated with disruption of normal structures and architectural morphology.

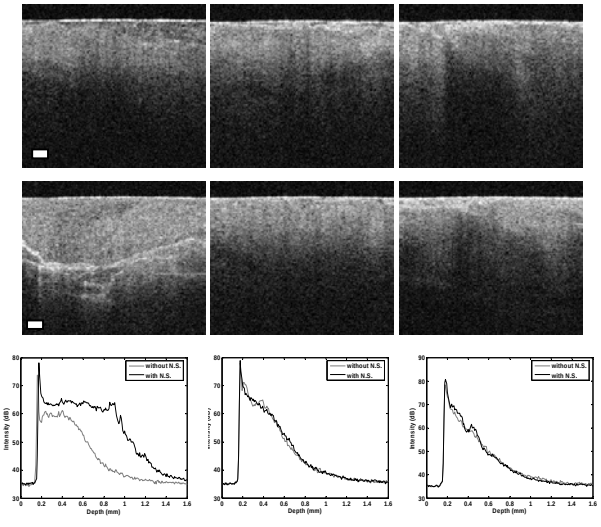

Figure 2: OCT imaging of Her2 expression *ex vivo*. Histologically Her2-positive breast cancer tissue before and after nanoshell addition (top row & middle row, respectively). Corresponding average A-scan images (bottom row). Scale bar is ~ 200 μm

From Figure 2, no significant OCT imaging contrast was observed in the malignant controls (top row of Figure 2). However, among the three discriminate groups (malignant control versus malignant tissue with Her2 conjugated nanoshells, with IgG conjugated nanoshells, and with bare nanoshells), significantly increased optical contrast was obtained in malignant tissue targeted with Her2 labeled nanoshells (left column, Figure 2). Other groups, on the other hand, show no differences before or after addition of nanoshells. To quantify the contrast among the samples, we calculated the averaged A-scan OCT intensity of each sample from 0 to 1.6 mm with an incremental depth of 8 μm. There is no significant intensity increases observed in normal tissue (bottom row of Figure 1). However, considerable intensity increase is obtained only in Her2 labeled nanoshells in malignant tissue (left column of Figure 2).

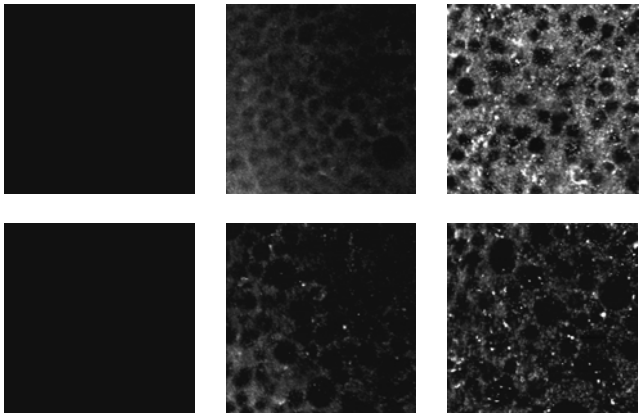

Figure 3: Reflectance confocal imaging of HER2 expression. HER2-positive SKBr3 (top row) or HER2-negative MCF7 (bottom row) cells were incubated with nanoshells labeled against HER2 (right column). A no nanoshell control and non-specific antibody control group are included for comparison purposes (left & middle columns).

Figure 3 shows the results of RCM images of HER2 positive SKBr3 and HER2 negative MCF7 cells with or without nanoshells within. Images shown in figure 3 were taken at the mid-focal plane at the same magnification and lighting conditions. Note that greater scatter-based contrast during imaging of HER2 expression in HER2 targeted cells (right column) compared to controls. Note also that no differences between HER2 negative cells targeted with either HER2 labeled or non-specifically labeled nanoshells (bottom row, middle, & right columns).

Figure 4 shows the results of RCM imaging of Her2 expression *ex vivo*. Middle and right-hand columns are of Her2-positive invasive carcinoma tissues. The left-hand column shows normal tissue. Top and bottom rows show tissues before and following nanoshell addition, respectively. Samples were exposed to either IgG (middle column) or Her2 labeled nanoshells (right-hand column). Compared to controls, greater contrast was observed in Her2-targeted tissues following addition of Her2 labeled nanoshells (bottom row, right-hand column).

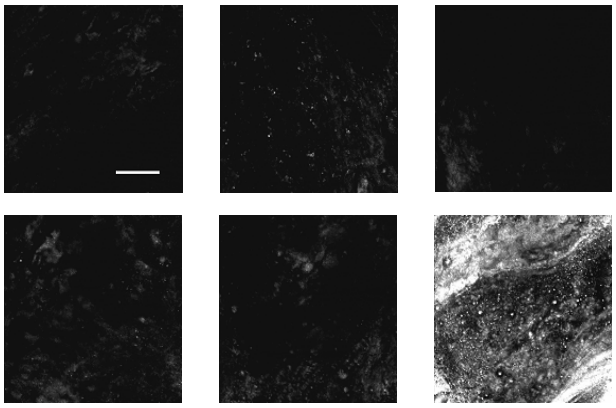

Figure 4: Reflectance confocal imaging of Her2 expression *ex vivo*. Histologically normal (left column) and Her2-positive breast cancer tissue (middle & right columns) before and after nanoshell addition (top & bottom rows, respectively). Scale bar is ~125 μm.

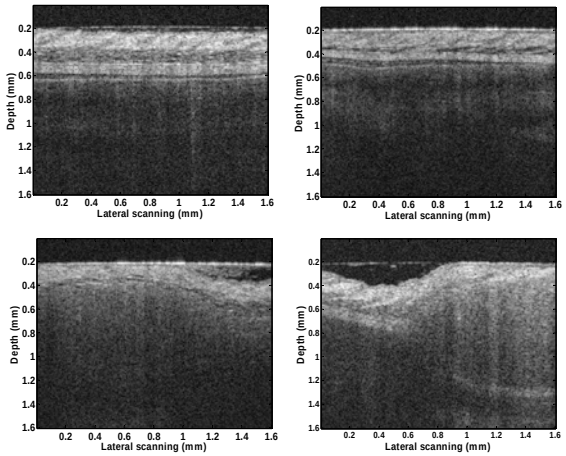

Figure 5: Optical Coherence Tomography imaging of tumor bearing mouse (First row) and non tumor bearing mouse (second row) *in vivo*. Clear image contrast was visible in image of nanoshell injected tumor bearing mouse (bottom, right column) contrary to the image of PBS injected tumor mouse.

To demonstrate the effect of nanoshells on in vivo OCT images, we performed OCT imaging over mouse tumor region. Nanoshells (0.1 ㎖, $5\times10^9/cm^3$)were injected into nonobese mouse tail vein.

In Figure 5, OCT images of tumor bearing mouse and non tumor bearing mouse were taken with and without nanoshells. In normal figures (top row), typical layered structure resulting from different refractive indices were shown. On the contrary, in tumor images (bottom row) no visible layer was appeared due to the destruction of tissue structure.

With nanoshells injection, tumor structure was clearly visible down to blood vessel compared to the tumor with PBS injection indicating that detectible light loss due to

NSTI-Nanotech 2007, www.nsti.org, ISBN 1420061836 Vol. 2, 2007

homogeneous tumor tissue can be greatly recovered by the scattering properties of gold nanoshells which accumulate into the tumor region.

In this paper, we demonstrate the potential of gold nanoshells as imaging contrast agents for optical based imaging modality. Nanoshells' tunable scattering property against various wavelengths as well as easy conjugation of antibodies on their surfaces gives a lot of imaging applications. These nanoparticles can also be broadly applied for other imaging and therapy applications by further varying core and shell sizes to optimize the optical properties.

ACKNOWLEDGEMENTS

We would like to acknowledge the support of this research by the National Science Foundation (BES 022-1544), National Science Foundation Center for Biological and Environmental Nanotechnology (EES-0118007), and the Department of Defense Congressionally Directed Medical Research Program (DAMD17-03-1-0384).

Author also would like to thank the partial finantial support by MIC and IITA.

REFERENCES

[1] D. Huang, E. A. Swanson, C. P. Lin, J. S. Stinson, W. Chang, M.R. Hee, T. Flotte, K. Gregory, C. A. Puliafito, and J. G. Fujimoto, Science, 254, 1178, 1991.

[2] R. Weissleder and U. Mahmood, Radiology, 219, 316, 2001.

[3] R. Weissleder, Nature Biotechnology, 19, 316, 2001

[4] S. L. Westscott, J. B. Jackson, C. Randloff, and N. J. Halas, Phy. Rev. Lett., B66, 155431, 2002.

[5] D.G. Duff and A. Baiker, Langmuir, 9, 2301, 1993